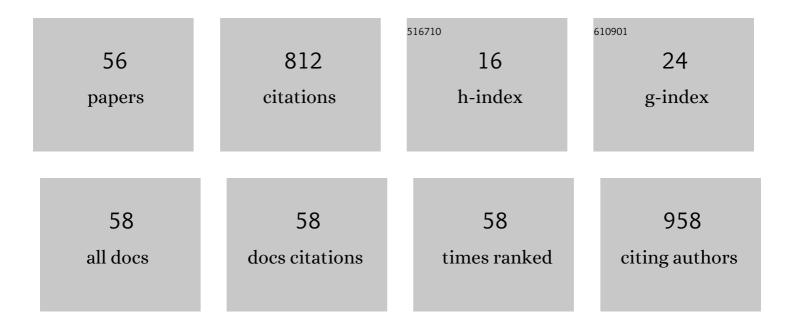
## Jia Zhuang

List of Publications by Year in descending order

Source: https://exaly.com/author-pdf/145458/publications.pdf Version: 2024-02-01



ΙΙΑ ΖΗΠΑΝΟ

#	Article	IF	CITATIONS
1	Enhanced Performance for Planar Perovskite Solar Cells with Samarium-Doped TiO <sub>2</sub> Compact Electron Transport Layers. Journal of Physical Chemistry C, 2017, 121, 20150-20157.	3.1	64
2	Effects of microstructure and pore water on electrical conductivity of cement slurry during early hydration. Composites Part B: Engineering, 2019, 177, 107435.	12.0	40
3	Negligible hysteresis planar perovskite solar cells using Ga-doped SnO2 nanocrystal as electron transport layers. Organic Electronics, 2019, 71, 98-105.	2.6	38
4	Analysis of interfacial nanostructure and interaction mechanisms between cellulose fibres and calcium silicate hydrates using experimental and molecular dynamics simulation data. Applied Surface Science, 2020, 506, 144914.	6.1	33
5	Preparation and property of 2â€acrylamideâ€2â€methylpropanesulfonic acid/acrylamide/sodium styrene sulfonate as fluid loss agent for oil well cement. Polymer Engineering and Science, 2012, 52, 431-437.	3.1	31
6	Regulated perovskite crystallinity via green mixed antisolvent for efficient perovskite solar cells. Organic Electronics, 2019, 69, 69-76.	2.6	31
7	Evolution of pore structure of oil well cement slurry in suspension–solid transition stage. Construction and Building Materials, 2019, 214, 382-398.	7.2	28
8	A novel tri-layered photoanode of hierarchical ZnO microspheres on 1D ZnO nanowire arrays for dye-sensitized solar cells. RSC Advances, 2015, 5, 16678-16683.	3.6	25
9	Interface Modification for Enhanced Efficiency and Stability Perovskite Solar Cells. Journal of Physical Chemistry C, 2020, 124, 12948-12955.	3.1	25
10	Strong Electron Acceptor of a Fluorine-Containing Group Leads to High Performance of Perovskite Solar Cells. ACS Applied Materials & Interfaces, 2021, 13, 41149-41158.	8.0	24
11	Research on the Interface Structure during Unidirectional Corrosion for Oil-Well Cement in H <sub>2</sub> S Based on Computed Tomography Technology. Industrial & Engineering Chemistry Research, 2016, 55, 10889-10895.	3.7	19
12	The coupled reaction and crystal growth mechanism of tricalcium silicate (C3S): An experimental study for carbon dioxide geo-sequestration wells. Construction and Building Materials, 2018, 187, 1286-1294.	7.2	19
13	Hydrothermal treatment of a TiO2film by hydrochloric acid for efficient dye-sensitized solar cells. New Journal of Chemistry, 2016, 40, 3233-3237.	2.8	18
14	Relationship Between the Microstructure/Pore Structure of Oil-Well Cement and Hydrostatic Pressure. Transport in Porous Media, 2018, 124, 463-478.	2.6	18
15	Formation and strengthening mechanisms of xonotlite in C3S-silica and C2S-silica powder systems under high temperature and pressure. Cement and Concrete Research, 2022, 157, 106812.	11.0	18
16	Synthesis and performance of itaconic acid/acrylamide/sodium styrene sulfonate as a self-adapting retarder for oil well cement. RSC Advances, 2015, 5, 55428-55437.	3.6	17
17	Interfacial modification using ultrasonic atomized graphene quantum dots for efficient perovskite solar cells. Organic Electronics, 2019, 75, 105415.	2.6	16
18	Effect of the hydration rate and microstructure of Portland cement slurry on hydrostatic pressure transfer. Powder Technology, 2019, 352, 251-261.	4.2	16

Jia Zhuang

#	Article	IF	CITATIONS
19	Enhanced performance of perovskite solar cells using DNA-doped mesoporous-TiO2 as electron transporting layer. Solar Energy, 2020, 206, 855-863.	6.1	16
20	Effect of different welding parameters on residual stress and deformation of 20/0Cr18Ni9 dissimilar metal arc-welding joint. Journal of Adhesion Science and Technology, 2020, 34, 1628-1652.	2.6	16
21	Multifunctional molecules of surfactant to support enhanced efficiency and stability for perovskite solar cells. Journal of Materials Science, 2020, 55, 14761-14772.	3.7	15
22	MAA-modified and luminescence properties of ZnO quantum dots. Science in China Series B: Chemistry, 2009, 52, 2125-2133.	0.8	14
23	Enhanced electron extraction using ZnO/ZnO-SnO2 solid double-layer photoanode thin films for efficient dye sensitized solar cells. Thin Solid Films, 2019, 684, 1-8.	1.8	14
24	Triphenylamine hydrophobic surface prepared by low-temperature solution deposition for stable and high-efficiency SnO2 planar perovskite solar cells. Journal of Alloys and Compounds, 2020, 830, 154710.	5.5	14
25	Effectiveness and microstructure change of alkali-activated materials during accelerated carbonation curing. Construction and Building Materials, 2021, 274, 122063.	7.2	14
26	Synergistic Defect Passivation for Highly Efficient and Stable Perovskite Solar Cells Using Sodium Dodecyl Benzene Sulfonate. ACS Applied Energy Materials, 2021, 4, 4910-4918.	5.1	14
27	Preparation and application of core–shell Fe3O4/polythiophene nanoparticles. Journal of Nanoparticle Research, 2011, 13, 6919-6930.	1.9	13
28	Improving the performance of lead acetate-based perovskite solar cells <i>via</i> solvent vapor annealing. CrystEngComm, 2019, 21, 4753-4762.	2.6	12
29	Self-healing mechanism of Zn-enhanced cement stone: An application for sour natural gas field. Construction and Building Materials, 2019, 227, 116651.	7.2	12
30	An intelligent natural fibrous membrane anchored with ZnO for switchable oil/water separation and water purification. Colloids and Surfaces A: Physicochemical and Engineering Aspects, 2022, 634, 128041.	4.7	12
31	Preparation of nano C-ZnO/SnO <sub>2</sub> composite photoanode via a two-step solid state reaction with high efficiency for DSSCs. RSC Advances, 2015, 5, 91997-92003.	3.6	11
32	TiO 2 photoanode surface modification via combined action of samarium and titanium salt in dye-sensitized solar cells. Solar Energy Materials and Solar Cells, 2017, 165, 45-51.	6.2	11
33	F4-TCNQ doped strategy of nickel oxide as high-efficient hole transporting materials for invert perovskite solar cell. Materials Science in Semiconductor Processing, 2021, 121, 105458.	4.0	11
34	Effects of Fe and Al ions during hydrogen sulphide (H2S)-induced corrosion of tetracalcium aluminoferrite (C4AF) and tricalcium aluminate (C3A). Journal of Hazardous Materials, 2021, 403, 123928.	12.4	11
35	A Versatile Organic Salt Modified SnO 2 Electron Transport Layer for Highâ€Performance Perovskite Solar Cells. Advanced Materials Interfaces, 2021, 8, 2100582.	3.7	11
36	The change and influence mechanism of the mechanical properties of tricalcium silicate hardening at high temperature. Construction and Building Materials, 2021, 308, 125065.	7.2	11

Jia Zhuang

#	Article	IF	CITATIONS
37	Mixed-phase Mesoporous TiO2 Film for High Efficiency Perovskite Solar Cells. Chemical Research in Chinese Universities, 2019, 35, 101-108.	2.6	10
38	One-step RF magnetron sputtering method for preparing Cu(In, Ga)Se2 solar cells. Journal of Materials Science: Materials in Electronics, 2018, 29, 11755-11762.	2.2	9
39	Crystallization of tricalcium silicate blended with different silica powder dosages at high temperature. Construction and Building Materials, 2022, 316, 125884.	7.2	9
40	Low-temperature dynamic vacuum annealing of ZnO thin film for improved inverted polymer solar cells. RSC Advances, 2017, 7, 29357-29363.	3.6	8
41	Enhanced ferroelectric and dielectric properties of BiFeO3–PbTiO3 thin films grown via a sol–gel multilayer deposition method. Journal of Sol-Gel Science and Technology, 2015, 75, 353-359.	2.4	7
42	Synthesis of microcrystalline brownmillerite Ca2(Al,Fe)2O5and its influence of mechanical properties to the class G oil-well cement. Journal of Adhesion Science and Technology, 2018, 32, 125-138.	2.6	7
43	Effect of red mud addition on oil well cement at high temperatures. Advances in Cement Research, 2021, 33, 28-38.	1.6	7
44	Resource utilization from solid waste originated from oil-based shale drilling cutting during shale gas development. Chemosphere, 2022, 298, 134318.	8.2	7
45	Structural evolution in micro-calcite bearing Ca-montmorillonite reinforced oilwell cement during CO2 invasion. Construction and Building Materials, 2022, 315, 125744.	7.2	5
46	Influence of laser power on the microstructure and properties of Fe314 alloy cladding layer on EA4T steel. Welding in the World, Le Soudage Dans Le Monde, 2022, 66, 1551-1563.	2.5	5
47	Terpolymerization and performance of 2â€acrylamideâ€2â€methyl propane sulfonic acid / itaconic acid / <i>N</i> â€vinylâ€2â€pyrrolidone. Journal of Applied Polymer Science, 2010, 117, 2951-2957.	2.6	4
48	Bilayer structured nanowire-array and nanotube-cluster TiO2 photoanode for efficient dye-sensitized solar cells. Chemical Research in Chinese Universities, 2015, 31, 412-417.	2.6	4
49	Synthesis and anti-corrosion performance of Adenine-L-Alanine ramification. Journal of Adhesion Science and Technology, 2016, 30, 851-865.	2.6	4
50	The influence of sulfomethyl phenol formaldehyde resin (SMP) on cementing slurry. Journal of Adhesion Science and Technology, 2015, 29, 1002-1013.	2.6	3
51	Multifunctional Additive of Potassium Cinnamate Improve Crystallization and Passivate Defect for Perovskite Solar Cell with Efficiency Exceeding 22%. Energy Technology, 0, , 2200125.	3.8	3
52	Preparation and Optical Properties of TiO2 Film with a Nest-Like Structure by Three Times of Circulating Hydrothermal Method. Nano, 2016, 11, 1650066.	1.0	2
53	Preparation of multistage sheet-cluster ZnO photoanode via a solid state reaction and its property in DSSCs. Chemical Research in Chinese Universities, 2016, 32, 437-442.	2.6	2
54	Efficient defect passivation for high performance perovskite solar cell by adding alizarin red S. Journal of Materials Science, 2021, 56, 19552-19563.	3.7	2

#	Article	IF	CITATIONS
55	Preparation and properties of optoelectronic conversion films of perovskite modified by octadecyl-trichloro silane. Organic Electronics, 2021, 88, 106028.	2.6	1
56	Strong connection between PVK and ETL induced by an anti-allergic agent interface for high-quality PSCs. Journal of Materials Science: Materials in Electronics, 2022, 33, 6456.	2.2	1